



Copyright © 2016 American Scientific Publishers
All rights reserved
Printed in the United States of America

Simulation and Parametrical Analysis of Highly Sensitive MEMS Based Piezoresistive Pressure Sensor

Kakali Das^{1a*}, Sunipa Roy^{2b}

¹Department of Electronics and Communication Engineering, St. Thomas College of Engineering and Technology, Kolkata, India

²Department of Electronics and Communication Engineering, Guru Nanak Institute of Technology, Kolkata, India

^{a*}*d.kakali.05@gmail.com*

^b*sunipa_4@yahoo.co.in*

Abstract: In this paper, a parametric analytical and simulation solution for highly sensitive MEMS based piezoresistive pressure sensor is proposed. The system output sensitivity of the pressure sensor is evaluated by interpreting the proper selection of diaphragm geometry of the square diaphragm and the position of piezoresistors. In order to achieve better sensor performance, the results of diaphragm deflection, stress profile and other effects are parametrically analyzed with the simulation using MATLAB programming. The range of applied pressure is considered from 5.333kPa (minimum value) to 39.997 kPa (maximum value). Blood pressure of human body should normally be less than 120/80 mm Hg (less than 120 systolic and less than 80 diastolic) for an adult age 20 or over. The sensor simulates the results for diaphragm deflection and induced stress for maximum and minimum measurable equivalent blood pressure of human body. Sensitivity of the sensor is influenced more powerfully by diaphragm thickness. Out of various diaphragm geometries, for a particular square silicon <100> diaphragm, the maximum deflection of 0.14 μm is found for an applied pressure of 39.997 kPa and the maximum stress of 25 MPa is achieved for the same applied pressure.

Keyword: MEMS; piezoresistor; pressure sensor; diaphragm; MATLAB.

1 INTRODUCTION

The measurement of pressure is an important part of many industrial and commercial systems. Specially, for building small pressure sensors, silicon has proven a wonderful material. When a pressure is applied on a thin silicon diaphragm, it is deflected; this deflection directs the stressing on the diaphragm on which very small piezoresistors are placed.

Micro Electro Mechanical systems (MEMS) is an incipient technology, which makes a great promise of market growth and new upcoming applications. In sensor design a simulation solution is one of the valuable processing. One of the major applications of the piezoresistive sensor is the silicon based pressure sensor. The modern technology of silicon piezoresistive pressure sensor is quite advanced and its accuracy in measurement is quite rigorous

in many of the advanced applications. Change in resistivity of a material resulting from an applied stress is the basic concept of piezoresistive effect. These pressure sensors are being used extensively in automobiles and process control [1]. Piezoresistive pressure sensors are very suitable for low pressure biomedical applications [2] not only for their small size but also relatively easy use and it's biocompatibility as well. Due to this reason this sensor has grown its popularity among designers. In designing of low-pressure sensors noise also needs to be considered especially for biomedical applications which requires high signal to noise ratio for errorless measurement of the low magnitude physiological signals [3].

In this paper, a perfect model of MEMS based piezoresistive pressure sensor is designed, in which four piezoresistors are symmetrically placed on the four sides of square diaphragm. Two piezoresistors are oriented to sense stress in the direction of their current axis and two are placed to sense stress perpendicular to their current flow. The piezoresistors are placed in a Wheatstone bridge connection, where V is bridge-input voltage, and ΔV is differential output voltage. The resistance change due to unbalanced bridge can directly convert into a voltage signal under an applied pressure. By applying Wheatstone bridge principle, with the increase of pressure, deflection on the diaphragm has been increased. These piezoresistors convert stresses induced in the silicon diaphragm by the applied pressure into a change of electrical resistance, which is then converted into voltage output by a Wheatstone bridge circuit as shown in Fig. 1

Fig. 1 shows the top view of a square diaphragm piezoresistive pressure sensor in which R1 and R3 are longitudinal and R2 and R4 are transverse piezoresistors forming a Wheatstone bridge with their axes aligned to $\langle 110 \rangle$ direction [4]. Further,

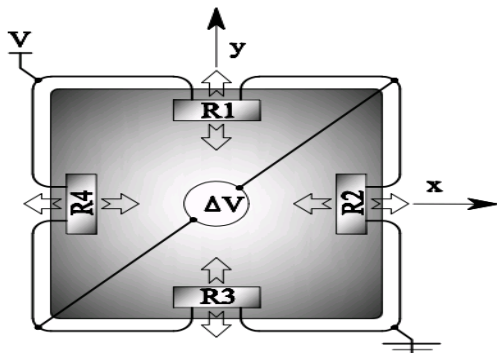


Fig. 1. Top view of conventional square diaphragm piezoresistive pressure sensor.

the longitudinal and transverse stresses both act on each resistor, *i.e.*, if a resistor experiences a stress σ_l length wise then it must also be subjected to a stress $\nu \cdot \sigma_l$ along its width and vice versa, where ν is the Poisson's ratio. Also, the stresses on the longitudinal resistors (R1 and R3), and on transverse resistors (R2 and R4) are equal but act in direction 90° to each other, that is, the transverse stress on R2 and R4 is the longitudinal stress on R1 and R3, and vice versa [5].

2 SENSOR DESIGN

Among variety of transducer effects, piezoresistivity is most popular, especially for electromechanical sensors produced by silicon material. The piezoresistive effect is given by,

$$\frac{\Delta R}{R} = \frac{\Delta \rho}{\rho} + (1 + 2\nu)\epsilon \quad (1)$$

Where ρ refers to resistivity of the material and usually given in $\Omega \cdot cm$, $\Delta \rho$ refers to change in resistivity of a piezoresistor. ρ depends on the doping concentration of the piezoresistors [6], ν is the Poisson's ratio and ϵ is the mechanical strain induced in the diaphragm.

The first part of the left hand side of equation 1 describes the piezoresistive effect and the second part defines the geometric effect. For piezoresistive materials like silicon, the piezoresistive effect dominates over geometric effect, so the second part of equation (1) is neglected and the linear piezoresistive effect is stated by the superposition of the longitudinal and the transverse piezoresistive effect with the stress components σ_l in longitudinal and σ_t in transverse direction and formulized as,

$$\frac{\Delta \rho}{\rho} = \frac{\Delta R}{R} = \pi_l \cdot \sigma_l + \pi_t \cdot \sigma_t \quad (2)$$

where, π_l and π_t refers to longitudinal and transverse piezoresistive coefficient, σ_l and σ_t refers to longitudinal and transverse stress. The effective value for the longitudinal piezoresistive coefficient and the transverse piezoresistive coefficient can be calculated from the piezoresistive coefficient tensor π_{ij} . Here π is the piezoresistive coefficient which depends on temperature, doping concentration and band structure [7]. π_l is the longitudinal piezoresistive coefficient and π_t is referred to as the transverse coefficient which can be expressed in terms of the basic piezoresistive coefficients π_{11} , π_{12} , and π_{44} . Denotation of contractive notation used for the piezoresistive coefficient π used as summarized in Table 1.

Table 1. Denotation of the contractive notation

Contractive notation	1	2	3	4	5	6
	x -	y -	z - z	y - z	x - z	x - y
Denotation	x	y		and	and	and y
				z - y	z - x	-x

By the contractive notation, the general piezoresistive coefficient π becomes a second rank tensor with 6×6 elements.

$$\pi_{ij} = \begin{bmatrix} \pi_{11} & \pi_{21} & \pi_{31} & \pi_{41} & \pi_{51} & \pi_{61} \\ \pi_{12} & \pi_{22} & \pi_{32} & \pi_{42} & \pi_{52} & \pi_{62} \\ \pi_{13} & \pi_{23} & \pi_{33} & \pi_{43} & \pi_{53} & \pi_{63} \\ \pi_{14} & \pi_{24} & \pi_{34} & \pi_{44} & \pi_{54} & \pi_{64} \\ \pi_{15} & \pi_{25} & \pi_{35} & \pi_{45} & \pi_{55} & \pi_{65} \\ \pi_{16} & \pi_{26} & \pi_{36} & \pi_{46} & \pi_{56} & \pi_{66} \end{bmatrix} \quad (3)$$

For anisotropic material, the number of independent components can be reduced due to symmetry effect. For example, in single-crystal silicon, there are only 12 non-zero coefficients instead of 36 [6]. Due to the cubic crystal symmetry, only three of them are independent those are π_{11} , π_{12} , and π_{44} .

For isotropic material, the number of independent components can be reduced to only two. The longitudinal and transverse piezoresistive coefficients of this sensor are:

$$\pi_l = \frac{1}{2}(\pi_{11} + \pi_{12} + \pi_{44}) \quad (4)$$

$$\pi_t = \frac{1}{2}(\pi_{11} + \pi_{12} - \pi_{44}) \quad (5)$$

where, $\pi_{11} = 6.6 \times 10^{-11} \text{ Pa}^{-1}$, $\pi_{12} = -1.1 \times 10^{-11} \text{ Pa}^{-1}$, and $\pi_{44} = 138.1 \times 10^{-11} \text{ Pa}^{-1}$ respectively.

The piezoelectric effects are shown as an illustration in Fig. 2. In Fig. 2(a), the resistor is stretched by the longitudinal force F in the same direction as the current flows, when a voltage is applied between the electrodes. Thus, the longitudinal piezoresistive effect has to be taken into account. In Fig. 2(b), the current flows perpendicular to the direction of the applied transverse force F constituting a transverse piezoresistive effect. Both structures can be easily build and used to characterize the different piezoresistive effects. The effective values for the longitudinal piezoresistive coefficient (π) and the transverse piezoresistive coefficient (π) can be

calculated from the piezoresistive coefficient tensor π_{ij} [6].

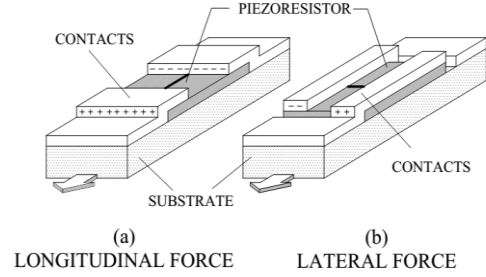


Fig. 2. The forces applied to the piezoresistor.

In this work, for this specific configuration of p-type diffused piezoresistors and tensile stress, the resistance of the resistors oriented in the longitudinal direction increases whereas the resistance of the resistors oriented in the transverse direction decreases. Thus both types of resistors can then contribute the linear relationship between output voltage and applied pressure. It increases the sensitivity of the pressure sensor.

The change of resistance reflects into a variation in the output voltage of the Wheatstone Bridge as given by the following Equation (6).

$$\frac{\Delta V}{V} = \frac{r}{(1+r)^2} \left\{ \frac{\Delta R_1}{R_1} - \frac{\Delta R_2}{R_2} + \frac{\Delta R_3}{R_3} - \frac{\Delta R_4}{R_4} \right\} \quad (6)$$

2.1 Stress-Strain Relation

For linear elastic, isotropy and plane stress conditions ($\sigma_z = \tau_{yz} = \tau_{zx} = 0$) stress-strain relations can be stated in the matrix form,

$$\begin{Bmatrix} \sigma_x \\ \sigma_y \\ \tau_{xy} \end{Bmatrix} = \frac{E}{1-\nu^2} \begin{bmatrix} 1 & \nu & 0 \\ \nu & 1 & 0 \\ 0 & 0 & \frac{1-\nu}{2} \end{bmatrix} \begin{Bmatrix} \varepsilon_x \\ \varepsilon_y \\ \gamma_{xy} \end{Bmatrix} \quad (7)$$

2.2 Kirchhoff's Plate Theory

Since the diaphragm thickness is very small like thin plate, Kirchhoff's Plate theory is applicable here. Transverse shear deformation is prohibited (Fig. 3), and the resulting expression is given by

$$\begin{Bmatrix} \sigma_x \\ \sigma_y \\ \tau_{xy} \end{Bmatrix} = -\frac{Ez}{1-\nu^2} \begin{bmatrix} 1 & \nu & 0 \\ \nu & 1 & 0 \\ 0 & 0 & \frac{1-\nu}{2} \end{bmatrix} \begin{Bmatrix} \frac{\partial^2 w}{\partial x^2} \\ \frac{\partial^2 w}{\partial y^2} \\ 2 \frac{\partial^2 w}{\partial x \partial y} \end{Bmatrix} \quad (8)$$

z is any arbitrary value from neutral axis in z -direction ($z=\pm t/2$). Thus the moment-curvature relations for a homogeneous and isotropic Kirchhoff plate are,

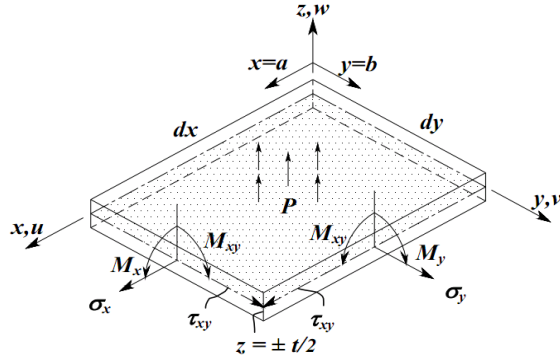


Fig. 3. Stresses and moments under the lateral force on differential element.

$$\begin{Bmatrix} M_x \\ M_y \\ M_{xy} \end{Bmatrix} = -D \begin{bmatrix} 1 & \nu & 0 \\ \nu & 1 & 0 \\ 0 & 0 & \frac{1-\nu}{2} \end{bmatrix} \begin{Bmatrix} \frac{\partial^2 w}{\partial x^2} \\ \frac{\partial^2 w}{\partial y^2} \\ 2 \frac{\partial^2 w}{\partial x \partial y} \end{Bmatrix} \quad (9)$$

where,

$$D = \frac{Et^3}{12(1-\nu^2)} \quad (10)$$

D is called *flexural rigidity* and analogous to flexural stiffness EI .

The state of deformation and stress throughout a Kirchhoff plate are completely described by a single field, namely lateral deflection $w=w(x,y)$ of the mid-surface. The differential equation of the deflection surface following the equilibrium equation is given by,

$$\frac{\partial^4 w}{\partial x^4} + 2 \frac{\partial^4 w}{\partial x^2 \partial y^2} + \frac{\partial^4 w}{\partial y^4} = \frac{P}{D} \quad (11)$$

For rectangular plate with all edges built in under uniformly distributed load, the maximum deflection and moments are given by,

$$w_{\max} = \alpha \frac{Pa^4}{D} \quad (12)$$

$$(M_x)_{\max} = \beta_1 Pa^2 \quad (13)$$

$$(M_y)_{\max} = \beta_2 Pa^2 \quad (14)$$

The Table 2 describes the values of α and β for varying the ratios of lengths of larger side to the smaller side of the rectangular diaphragm.

For square plate, $a=b=L$, the maximum deflection and moments and stresses are,

$$w_{\max} = 0.01512(1-\nu^2) \frac{Pa^4}{Et^3} \quad (15)$$

$$(M_x)_{\max} = (M_y)_{\max} = 0.0513Pa^2 \quad (16)$$

The maximum induced stress on the square diaphragm is given by,

$$\sigma_{\max} = 6 \frac{(M_{x \text{ or } y})_{\max}}{t^2} = 0.308 \frac{Pa^2}{t^2} \quad (17)$$

Table 2. Coefficients α , β_1 , β_2 for varying b/a ratios.

b/a	1.0	1.2	1.4	1.6	∞
α	0.00126	0.00172	0.00207	0.0023	0.0026
β_1	0.0513	0.0639	0.0726	0.0780	0.0833
β_2	0.0513	0.0554	0.0568	0.0571	0.0571

2.3 Parallel-Normal Combination of Piezoresistors

If the piezoresistor is parallel to the edge: The ratio of change in resistance to the total resistance corresponding to the piezoresistor is given by,

$$\frac{\Delta R}{R} = \pi_l \cdot \sigma_l + \pi_t \cdot \sigma_t = (\pi_t - \nu \pi_l) \sigma_{\max} \quad (18)$$

If the piezoresistor is normal to the edge: The equation becomes,

$$\frac{\Delta R}{R} = \pi_l \cdot \sigma_l + \pi_t \cdot \sigma_t = (\pi_l - \nu \pi_t) \sigma_{\max} \quad (19)$$

Therefore, according to the specific diaphragm, the equation for differential output voltage has been changed to

$$\frac{\Delta V}{V} = \frac{r}{(1+r)^2} (\pi_l - \nu \pi_t) \sigma_{\max} \quad (20)$$

And Sensitivity 'S' of the sensor is given by,

$$S = \frac{\Delta V}{P} \quad (21)$$

3 PARAMETRIC STUDY

The Wheatstone bridge is balanced under the condition of Zero- pressure. When a pressure is applied to the diaphragm, all the piezoresistors undergo a change in resistance and the change of resistance affects the output voltage of the Wheatstone bridge. From the simulation, it is

observed that by changing the piezoresistor positions as well as silicon diaphragm geometries, the diaphragm having smaller thickness with the piezoresistors placed at the center of the edges of each side reflects comparatively better sensitivity. Table 3 shows the mechanical properties of the components of the sensor. The Table 4 shows the case study of different dimensions of the square diaphragm on which pressure is applied. Also the sensitivity is calculated corresponding to each diaphragm as shown in Table 4.

Table 3. Specification of piezoresistor and diaphragm.

Max. Pressure (P)	Poisson's ratio (ν)	Young's modulus (E)	Density (ρ)	Diaphragm material	Piezoresistive material
39.997 KPa	0.28	160 GPa	2330 kg/m ³	Silicon (p type)	Poly Silicon

Table 4. Square Diaphragm Dimensions and sensitivity analysis under input voltage 5 volts and applied pressure up to 39.997 kPa.

Edge(a) in μm	448	455	463
Thickness(t) in μm	10	15	20
Sensitivity in μV/Pa	0.698	0.320	0.186

The study about sensitivity of the sensor as shown in Table 4 indicates that the value of sensitivity is higher for the diaphragm having smaller area and smaller thickness.

The Fig. 4 shows that the three different types of silicon diaphragms deflect differently upon the application of same amount of pressure. From the analysis, it is seen that the diaphragm having comparatively smaller area and smaller thickness shows maximum deflection. For the square diaphragm of length 448 μm and thickness of 10 μm shows maximum deflection about 0.14 μm for the maximum applied pressure of 39.997 kPa.

The Fig. 5 shows the stress profile for square diaphragms of different dimensions. It is observed that the maximum stress induced for the maximum applied pressure for the diaphragm for which the ratio of its length to thickness is maximum. Here the ratios are 44.8 (=448/10), 30.33 (=455/15), 23.15 (=463/20). It is evident from the stress profile, that the maximum stress induced for the diaphragm of length 448 μm and of thickness of 10 μm.

It is visualised from the Fig. 6 that the nature of the

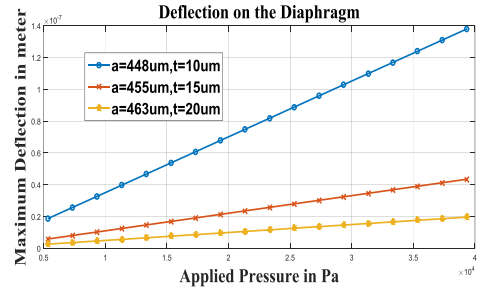


Fig. 4. Variation of maximum deflection with different sizes of square diaphragms with the applied pressure.

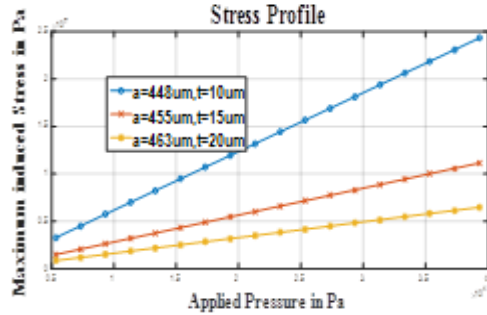


Fig. 5. Plot of Maximum induced stress on the diaphragm Vs. applied pressure.

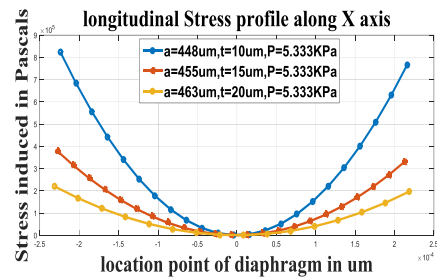


Fig. 6. Longitudinal stress profile along X= ±(l/2) for highly sensitive MEMS based piezoresistive pressure sensor.

stress profiles are fairly similar for the square diaphragms having different dimensions along y axis. The maximum longitudinal tensile stress is experienced at the edges and the maximum compressive stress is obtained at the centre. So, it is noticed that maximum stress is induced at the centre of the edges of the diaphragm and accordingly the piezoresistors are placed to obtain maximum sensitivity.

4 CONCLUSION

In this paper, the investigation using MATLAB programming clearly indicates the outcome of using of different diaphragm dimensions and the position of piezoresistors. The maximum stress was induced at the centre of the edges of the diaphragm and accordingly the piezoresistors were placed to obtain maximum sensitivity. The diaphragm having comparatively smaller area and smaller thickness

showed maximum deflection. The induced stress was found highest with the maximum applied pressure where the ratio of the diaphragm length to thickness was maximum. Out of the three diaphragm dimensions used here, it was optimized that the diaphragm having smaller area and smaller thickness can be used as highly sensitive pressure sensor.

REFERENCES

- [1] W. J. Eaton and J. H. Smith, 1997. Micro machined pressure sensors: review and recent developments, *Smart Materials and Structures*, vol. 6, pp. 530-539.
- [2] S. Marco, J. Samitier, O. Ruiz, J. R. Morante, J. E. Steve, 1996. High performance piezoresistive pressure sensors for biomedical applications using very thin structured membranes, *Meas. Sci and Technol.*, vol. 7, pp. 1195-1203.
- [3] P. Steiner and W. Lang, 1995. Silicon nitride membrane sensors with monocrystalline transducers, *Sensors and Actuators B*, pp. 71-75.
- [4] Y. Kanda, 1997. Optimum Design Considerations for Silicon Piezoresistive Pressure Sensor, *Sensor and Actuators. A*, vol. 62, pp. 539-542.
- [5] H. S. Ko, 2007. Novel fabrication of a pressure sensor with polymer material and evaluation of its performance, *J. Micromech. Microeng*, vol. 17, pp. 1640-1648.
- [6] P. S. Roy and M. Chattopadhyay, 2014. A simulation based geometrical analysis of MEMS capacitive pressure sensors for high absolute pressure measurement, *IJETAE*, vol. 4, spl issue 7.
- [7] B. Abdelaziz, K. Fouad, and S. Kemouche, 2014. The effect of temperature and doping level on the characteristics of piezoresistive pressure, *Journal of sensor technology*, vol. 4, no. 2, pp. 59-65.